

Detecting and Characterizing the Fluxionality in Pt Nanoparticles

Advait Gilankar^{1*}, Benjamin K. Miller², Adrià Marcos Morales³, Piyush Haluai¹, Mai Tan¹, Joshua L. Vincent¹, Carlos Fernandez-Granda³ and Peter A. Crozier¹

¹. Arizona State University, Tempe, AZ, United States.

². Gatan, Inc. Pleasanton, CA, United States.

³. New York University, New York, United States.

* Corresponding author: agilanka@asu.edu

Platinum on ceria support is a technologically important and highly active catalyst for CO oxidation [1–3]. Past studies have shown that the functioning of this catalyst is influenced by structural rearrangements (fluxionality) occurring under reaction conditions [4]. Our latest *in situ* TEM results on this catalyst show significant fluxionality exhibited by Pt nanoparticles even at room temperature in a CO atmosphere. Correlating fluxionality and catalytic activity will provide fundamental insights into the reaction pathways and help in the design of better catalysts. The fluxionality is often stochastic with the particles showing periods of structural stability punctuated with periods of intense structural rearrangement. In this work we discuss an approach to detect the onset of unstable behavior of Pt nanoparticles on ceria exposed to CO gas of different partial pressures at room temperature.

Atomic resolution time-resolved image series of Pt/ CeO₂ nanoparticles were acquired under varying CO partial pressures on an aberration-corrected FEI Titan environmental transmission electron microscopy (ETEM) operated at 300 kV. The *in situ* images were recorded using the Gatan K3 IS camera in CDS mode at 75 frames per second (fps). The state-of-the-art direct detection cameras allows temporal resolution of up to $\sim 10^{-3}$ s. However, the signal-to-noise ratio is degraded due to limited beam intensity and low exposure time per frame [5, 6]. The basic approach that we initially tried in detecting the changes in the structural re-arrangements was subtracting the 2 adjacent frames and looking at the residual. This approach fails because of high noise present in the images. Handling the extremely noisy dataset required a more sophisticated approach to event detection based on an exponentially weighted moving average (EWMA) method to detect significant changes in the image signal in time. Exponentially weighted moving average (EWMA) is a widely used technique for smoothing out random fluctuations in a time series dataset by averaging with exponentially decaying weighting factors [7]. To determine the optimum approach for detection of structural dynamics, we tested several different implementations of EWMA. We used 2 different weighting factors (applied in exponentially decaying manner backwards in time) and performed the absolute difference of those EWMA (called as ‘EWMA Backward’). In a similar manner we compute ‘EWMA Forward’, placing exponentially decaying weights for the data ahead of time. We further subtracted EWMA Backward from EWMA Forward and used the derivative of the difference between 2 EWMA for pinpointing the exact time to locate the changes in the signal.

A time dependent step function is shown to demonstrate the working the principle of EWMA. **Figure 1 (a)** shows the function used for testing the algorithm, **Figure 1 (b), (c)** show the EWMA Backward and EWMA Forward respectively, **Figure 1 (d), (e)** show subtraction of EWMA Backward from EWMA Forward and the derivative of the difference. We demonstrate the application of same approach on detecting fluxionality on Pt particles using the experimental data in **Figure 2**. We considered a region on the Pt nanoparticle and applied the technique shown in **Figure 1(e)**. To apply the technique described in

Figure 1(e), we consider a region on the Pt nanoparticle of 100 x 100 pixels. We sum the squared values of the pixels in that region and normalize it with the area to obtain a number which we refer to as ‘Fluxionality Coefficient’. **Figure 2 (a)** demonstrates the plot of ‘Fluxionality Coefficient’ versus Frame Number. **Figure 2 (b)-(e)** show the noisy experimental images around the peak corresponding to the frame number 908. As, it is very difficult to see structural differences in the noisy images, to denoise the experimental images we have used an Unsupervised Deep Video Denoiser (UDVD) [8]. **Figure 2 (f)-(i)** display the denoised images by applying the unsupervised neural network, which easily show the fading of the fringes in Pt nanoparticle in the frame 908 (as indicated by figure 2 (a)). From the results demonstrated in **Figure 2**, we see this EWMA framework can detect the subtle structural rearrangements in nanoparticles under catalytic conditions and can be used on large *in situ* TEM datasets captured at high-temporal resolution [9].

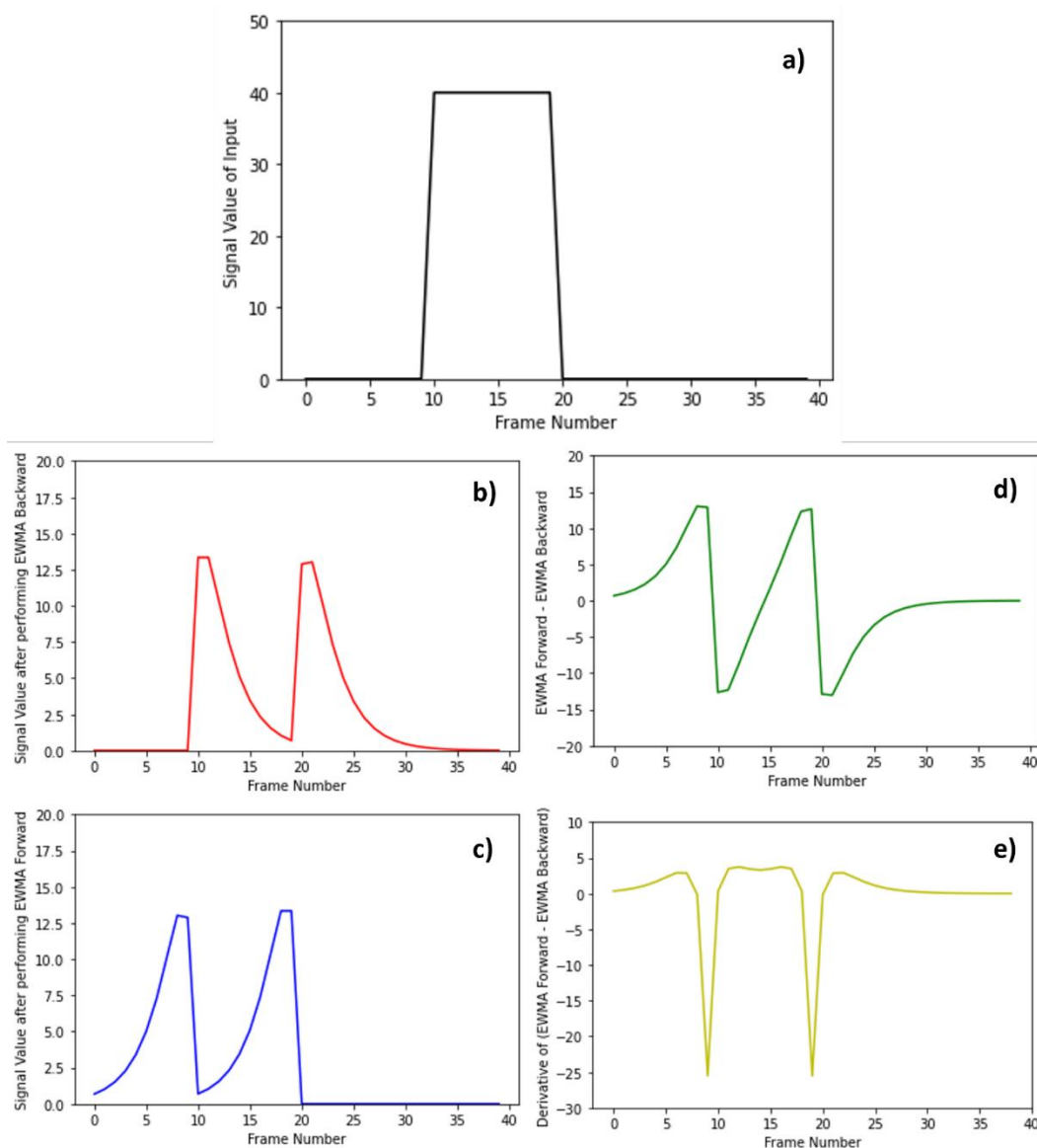


Figure 1. (a) Represents the ‘time-step’ signal value used for testing the algorithm. (b) and (c) represent the ‘EWMA Backward’ and ‘EWMA Forward’ respectively. (d) shows the difference between EWMA Forward and EWMA Backward. (e) shows the derivative of the difference computed in (d).

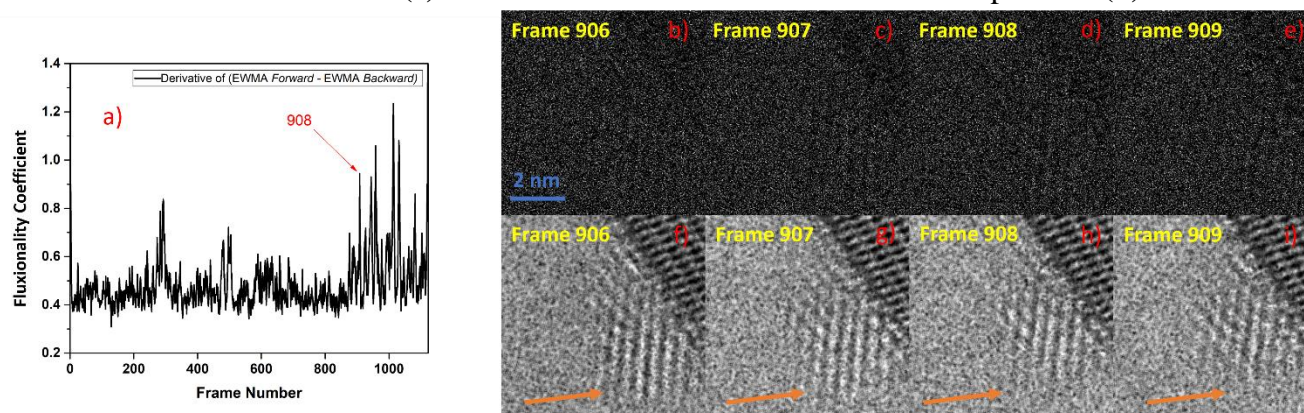


Figure 2. (a) Displays the plot between the fluxionality coefficient and frame number (after applying the EWMA Derivative method). (b)-(e) shows the noisy experimental image time-series on which the algorithm is applied. (f)-(i) represent the images with improved SNR obtained after denoising the experimental dataset showing the fluxionality of Pt nanoparticles.

References:

- [1] JL Vincent et al., *Nature Communications* **12** (2021), p. 5789.
- [2] Y Lu et al., *ChemCatChem* (**12**)6, pg. 1726.
- [3] X Ye et al., *Nano Research* (**12**)6 (2019), p. 1401.
- [4] EL Lawrence et al., *ACS Nano* (**15**)2 (2021), p. 2624.
- [5] R Manzorro et al., *Microscopy and Microanalysis* **27**(S1), p. 1306.
- [6] JL Vincent et al., *Microscopy and Microanalysis* (**27**)6, p. 1431.
- [7] MB Perry in “Wiley Encyclopedia of Operations Research and Management Science” (2010).
- [8] DY Sheth et al. arXiv:2011.15045v3 [eess.IV]
- [9] We gratefully acknowledge the support of the following NSF grants (OAC 1940263, OAC 1940097, CBET 1604971 and DMR 184084). We also acknowledge the support from DOE grant BES DE-SC0004954. The authors acknowledge HPC resources available through ASU, and NYU as well as the John M. Cowley Center for High Resolution Electron Microscopy at Arizona State.